Kuroiwa N, Abematsu N, Matsuo Y, Nakao K, Sakamoto T	[A case of intraocular lymphoma having retinal adverse events associated with intravitreal methotrexate].	Nihon Ganka Gakkai Zasshi	115(7)	611-6	2011
Matsuo Y, Uemura A, Nakano T, Inoue M, Sakamoto T	Atypical presentation of acute macular neuroretinopathy with tiny parafoveal reddish-brown lesions	Jpn J Ophthalmol	55(4)	362-4	2011
Ueno Y, Sonoda S, Suzuki R, Yokouchi M, Kawasoe Y, Tachibana K, Maruyama K, Sakamoto T, Komiya S	Combination of ultrasound and Bubble liposome enhance the effect ofdoxorubicin and inhibit murine osteosarcoma growth	Cancer Biol Ther	15;12(4)	270-7	2011
Yoshinaga N, Arimura N, Otsuka H, Kawahara KI, Hashiguchi T, Maruyama I, Sakamoto T	NSAIDs inhibit neovascularization of choroid through HO-1-dependent pathway	Lab Invest	91(9)	1277-90	2011
Kamisasanuki T, Tokushige S, Terasaki H, Khai NC, Wang Y, Sakamoto T, Kosai K	Targeting CD9 produces stimulus-independent antiangiogenic effects predominantly in activated endothelial cells during angiogenesis: A novel antiangiogenic therapy.	Biochem Biophys Res Commun	413(1)	128-35	2011
Asaoka R, Crabb DP, Yamashita T, Russell RA, Wang YX, Garway-Heath DF	Patients Have Two Eyes: Binocular versus Better Eye Visual Field Indices.	Invest Ophthalmol Vis Sci	52(9)	7007-11	2011
Nakano T, Uemura A, Sakamoto T	Incidence of iatrogenic peripheral retinal breaks in 23-gauge vitrectomy for macular diseases	Retina	31(10)	1997-2001	2011
Yamakiri K,Sakamoto T	Earlydiagnosis of macular hole closure of a gas-filled eye with Watzke-Allen slit beam test and spectral somain optical coherence tromography	Retina	epub	[Epub ahead of print]	2011

Kamisasanuki T, Uchino E, Sakamoto T	Choroidal neovascularization of optic disk melanocytoma treated with bevacizumab	Eur J Ophthalmol	epub	[Epub ahead of print]	2011
Yokoi T, Umezawa T, Azuma N	Establishment of functioning human corneal endothelial cell line with high growth potential	PLos ONE	7(1)	e29677	2012
Seko Y, Azuma N, Umezawa A,	Identification of factors determining human photoreceptor cell fate	PLos ONE		In press	2011
Nishina S、Suzuki Y, Yokoi T, Kobayashi Y, Noda E, Azuma N	Clinical features of congenital retinal folds	Am J Ophthalmol	153(1)	81-7	2012
Yamasaki1 T, Kawasaki H, Arakawa S, Shimizu K, Shimizu S, Reiner O, Okano H, Nishina S, AzumaN, Penninger JM, Katada T, Nishina H.	Stress-activated protein kinase MKK7 regulates axon elongation in the developing cerebral cortex.	Journal of Neuroscience	31	16872–16883	2011
Shigeyasu C, Yamada M, Mizuno Y, Yokoi T, Nishina S, Azuma N.	Clinical features of anterior segment dysgenesis associated with congenital corneal opacities	Cornea		[Epub ahead of print]	2011
Kobayashi Y, Yokoi T, Yokoi T, Hiraoka H, Nishina S, Azuma N.	Fluorescein staining of the vitreous during vitrectomy for retinopathy of prematurity.	Retina	31	1717-1719	2011
Sawada M, Sato M, Hikoya A, Wang C-X, Minoshima S, Azuma N, Hotta Y.	A case of aniridia with uniocular Peters anomaly	J AAPOS	15	104-106	2011

Kaneko H, Suzutani T, Aoki K, Kitaichi N, Ishida S, Ishiko H, Ohashi T, Okamoto S, Nakagawa H, Hinokuma R, Asato Y, Oniki S, Hashimoto T, Iida T, Ohno S	Epidemiological and virological features of epidemic keratoconjunctivitis due to new human adenovirus type 54 in Japan	Br J Ophthalmol	95	32-36	2011
Maruko I, Iida T, Sugano Y, Oyamada H, Sekiryu T, Fujiwara T, Spaide RF	Subfoveal choroidal thickness after treatment of Vogt-Koyanagi-Harada disease	Retina	31	510-517	2011
Imamura Y, Iida T, Maruko I, Zweifel SA, Spaide RF.	Enhanced depth imaging optical coherence tomography of the sclera in dome-shaped macula	Am J Ophthalmol	151	297-302	2011
Tano Y, Ohji M; EXTEND-1 study group (Iida T, Ishibashi T, Ishida S, Kishi S, Ohji M, Okada AA, Sato Y, Shiraga F, Shiraki K, Tano Y, Terasaki H, Yuzawa M)	Long-term efficacy and safety of ranibizumab administered pro re nata in Japanese patients with neovascular age-related macular degeneration	Acta Ophthalmol	89	208-217	2011
Tano Y, Ohji M, EXTEND-I Study Group	Long-term efficacy and safety of ranibizumab administered pro re nata in Japanese patients with neovascular age-related macular degeneration in the EXTEND-I Study	Acta Ophthalmol (Reprinted from Early View article)		1-10	2011
Nakata I, Yamashiro K, Yamada R, Gotoh N, Nakanishi H, Hayashi H, Tsujikawa A, Otani A, Saito M, Iida T, Oishi A, Matsuo K, Tajima K, Matsuda F, Yoshimura N	Association between he SERPING1 gene and neovascular age-related macular degeneration and polypoidal choroidal vasculopathy in Japanese	PLos ONE	6:e	19108	2011

Nakata I, Yamashiro K, Yamada R, Gotoh N, Nakanishi H, Hayashi H, Tsujikawa A, Otani A,Ooto A, Tamura H, Saito M, Saito K, Iida T, Oishi A, Kurimoto Y, Matsuda F, Yoshimura N.	Genetic variants in pigment epithelium-derived factor influence response of polypoidal choroidal vasculopathy to photodynamic therapy	Ophthalmology	118	1408-1415	2011
Maruko I, Iida T, Ojima A, Sekiryu T	Subretinal dot-like precipitates and yellow material in central serous chorioretinopathy	Retina	31	759-765	2011
Maruko I, Iida T, Sugano Y, Saito M, Sekiryu T	Subfoveal retinal and choroidal thickness after verteporfin photodynamic therapy for polypoidal choroidal vasculopathy	Am J Ophthalmol	151	594-603	2011
Ojima A, Iida T, Sekiryu T, Maruko I, Sugano Y	Photopigments in central serous chorioretinopathy	Am J Ophthalmol	151	940-952	2011
Maruko I, Iida T, Sugano Y, Ojima A, Sekiryu T	Subfoveal choroidal thickness in fellow eyes of patients with central serous chorioretinopathy	Retina	31	1603-1608	2011
Ikuno Y, Maruko I, Yasuno Y, Miura M, Sekiryu T, Nishida K, Iida T	Reproducibility of retinal and choroidal thickness measurements in enhanced depth imaging and high-penetration optical coherence tomography	Invest Ophthalmol Vis Sci	52	5536-5540	2011
Saito M, Iida T, Kano M	Intravitreal ranibizumab for polypoidal choroidal vasculopathy with recurrent or residual exudation	Retina	31	1589-1597	2011
Sekiryu T, Oguchi Y, Arai S, Wada I, Iida T	Autofluorescence of the cells in human subretinal fluid.	Invest Ophthalmol Vis Sci	52	8534-8541	2011

Maruko I, Iida T, Sugano Y, Furuta M, Sekiryu T	One-year result of choroidal thickness following photodynamic therapy in central serous chorioretinopathy	Retina		[Epub ahead of print]	2011
Toju R, Iida T, Sekiryu T, Saito M, Maruko I, Kano M	Near-infrared autofluorescence in patients with idiopathic submacular choroidal neovascularization	Am J Ophthalmol	153(2)	314-9	2012
Maruko I, Iida T, Sugano Y, Oyamada H, Sekiryu T	Morphologic choroidal and sclera changes at the macula in tilted disc syndrome with staphyloma using optical coherence tomography	Invest Ophthalmol Vis Sci	52(12)	8763-8	2011
Yamashiro K, Mori K, Nakata I, Tsuchihashi T, Horie-Inoue K, Nakanishi H, Tsujikawa A, Saito M, Iida T, Yamada R, Matsuda	Association of elastin gene polymorphism to age-related macular degeneration and polypoidal choroidal vasculopathy	Invest Ophthalmol Vis Sci	52(12)	8780-4	2011
Saito M, Iida T, Kano M	Combined intravitreal ranibizumab and photodynamic therapy for polypoidal choroidal vasculopathy	Retina		In press	2011
Saito M, Iida T, Kano M	Combined intravitreal ranibizumab and photodynamic therapy for retial angiomatous proliferation	Am J Ophthalmol	153(3)	504-514	2012
Saito M, Iida T, Kano M	Intravitreal ranibizumab for exudative age-related macular degeneration with good baseline visual acuity.	Retina		In press	2011
Maruko I, Iida T, Sugano Y, Ojima A, Oyamada H, Sekiryu T	Demographic features of idiopathic macular telangiectasia in Japanese patients	Jpn J Ophthalmol		[Epub ahead of print]	2011
飯田知弘	眼画像診断の進歩　黄斑疾患の病態ー画像診断による形態と機能解析—	日眼会誌	115	238-275	2011

齊藤かおり, 森 隆史, 根津吉史, 清野あかね, 坂本章子, 丹治弘子, 橋本禎子,八子恵子, 飯田知弘.	レチノマックス®で測定した3歳児の屈折値(3歳児検診での測定結果から).	日本視能訓練士協会誌	39	159 -164	2011
森 隆史, 齊藤かおり,坂本章子, 丹治弘子, 橋本禎子,八子恵子, 飯田知弘.	3歳児検診要精査児の視力と屈折値	眼科臨床紀要	4	240 -244	2011
齊藤かおり, 森 隆史,清野あかね,丹治弘子, 橋本禎子,八子恵子, 飯田知弘.	3歳児のレチノマックス®を用いた屈折検査での調節介入.	眼科臨床紀要	4	245 -248	2011

総説

発表者氏名	論文タイトル名	発表誌名	巻号	ページ	出版年
飯田知弘,石橋達朗	黄斑疾患アップデート	あたらしい眼科	28	155 -156	2011
丸子一朗,飯田知弘	黄斑疾患の脈絡膜OCT	あたらしい眼科	28	225 -231	2011
齋藤昌晃	網膜血管腫状増殖に対する治療戦略	眼科手術	24	26 -34	2011
森 隆史	眼瞼の形成	眼科手術	24	308 -312	2011
丸子一朗	Enhanced Depth Imaging と中心性漿液性脈絡網膜症の脈絡膜OCT所見.	あたらしい眼科	28	1244-1248	2011
齊藤かおり, 森隆史, 根津吉史, 清野あかね, 坂本章子, 丹治弘子, 橋本禎子,八子恵子;飯田知弘	レチノマックス®で測定した3歳児の屈折値(3歳児検診での測定結果から)	日本視能訓練士協会誌	39	159 -164	2011
森 隆史, 齊藤かおり,坂本章子, 丹治弘子, 橋本禎子,八子恵子, 飯田知弘	3歳児検診要精査児の視力と屈折値	眼科臨床紀要	4	240 -244	2011
齊藤かおり, 森隆史,清野あかね, 丹治弘子, 橋本禎子,八子恵子, 飯田知弘	3歳児のレチノマックス®を用いた屈折検査での調節介入	眼科臨床紀要	4	245 -248	2011

Clinical Ophthalmology

Dovepress
open access to scientific and medical research

Open Access Full Text Article

ORIGINAL RESEARCH

Detection of photoreceptor disruption by adaptive optics fundus imaging and Fourier-domain optical coherence tomography in eyes with occult macular dystrophy

Yoshiyuki Kitaguchi[1]
Shunji Kusaka[1]
Tatsuo Yamaguchi[2]
Toshifumi Mihashi[2]
Takashi Fujikado[1]

[1]Department of Applied Visual Science, Osaka University Graduate School of Medicine, Osaka, Japan; [2]Topcon Research Institute, Itabashi, Japan

Purpose: To investigate the structural changes in the photoreceptors by adaptive optics (AO) fundus imaging and Fourier-domain optical coherence tomography (FD-OCT) in eyes with occult macular dystrophy (OMD).

Design: Observational case reports.

Methods: Eight eyes of four patients who were diagnosed with OMD were examined. All eyes had a complete ophthalmological examination. Multifocal electroretinograms (mfERGs) were recorded from all eyes. AO and FD-OCT images of foveal photoreceptors were obtained.

Results: The best-corrected visual acuity (BCVA) of these eyes ranged from 20/20 to 20/200, and the ocular fundus was normal by conventional ocular examination in all eyes. The amplitudes of the mfERGs were decreased in the foveal area. The inner and outer segment (IS/OS) junction of the photoreceptors in the foveal area was disrupted. The IS/OS junction was intact in one eye with a BCVA of 20/20, and the outer segment layer between the IS/OS junction and retinal pigment epithelium of the FD-OCT images was identified only in the center of the fovea. The AO images showed patchy dark areas in all eyes, which indicated a disruption of the mosaic of bright spots in the fovea.

Conclusion: Structural changes of photoreceptors in OMD patients were detected tangentially by FD-OCT and en face by AO.

Keywords: Photoreceptors, OMD, images, retinal imaging

Introduction

Occult macular dystrophy (OMD) is a progressive hereditary macular dystrophy which is characterized by reduced visual acuity with an essentially normal fundus and normal fluorescein angiography.[1] Full-field electroretinograms (ERGs) are normal in OMD patients, and only the focal macular ERGs and multifocal ERGs (mfERGs) recorded from the macular area are reduced.[2,3]

With advances in retinal imaging, it has become easier to detect anatomical changes of the retina in eyes with OMD. Thus, Kondo et al reported a reduction of the retinal foveal thickness measured by time domain optical coherence tomography (OCT) in OMD patients,[4] and Brockhurst et al reported a thinning of the outer nuclear layer that was measured by Stratus OCT in OMD patients.[5] Although the main site of the lesion appeared to be the photoreceptor layer, abnormalities of the photoreceptors have not been reported in imaging studies. This deficiency is probably because of the low axial and transverse resolution of the imaging instruments.

Correspondence: Takashi Fujikado
Department of Applied Visual Science, Osaka University Graduate School of Medicine, 2-2 Yamadaoka, Suita, Osaka 565-0871, Japan
Tel +81 6 6879 3941
Email fujikado@ophthal.med.osaka-u.ac.jp

submit your manuscript | www.dovepress.com
Dovepress
DOI: 10.2147/OPTH.S17335

The axial resolution of the Fourier-domain OCT (FD-OCT) is approximately 6 μm, which is significantly better than the 10 μm of standard OCTs. The external limiting membrane (ELM) (first highly reflective line), photoreceptor inner and outer segment junction (IS/OS) (second line), and the retinal pigment epithelium (RPE) (fourth line) can all be detected with an FD-OCT.[6–9] Disturbances of the IS/OS junction have been reported in some retinal diseases, eg, postoperative retinal detachment, central serous chorioretinopathy, and retinal dystrophy, which could not be detected ophthalmoscopically.[7,10–13] A disruption of the third highly reflective line of the FD-OCT images has been reported in cases of macular microhole.[13] Because the third line is considered to represent the outer segment of the photoreceptors because of its anatomical position, the disruption suggests an alteration of the photoreceptor outer segments. However, the origin of the third line has not been well investigated.

The adaptive optics (AO) fundus camera can obtain images with a transverse resolution of <2 μm, which makes it possible to resolve individual photoreceptors in living human eyes.[14–20] An increase in the cone spacing in retinas with cone dystrophy can be detected by AO imaging,[20,21] and the degree of the increased spacing is consistent with the decrease in visual function measured by mfERGs.[22] A disruption of the third bright line of the FD-OCT images is reported to cause a dark area in the AO fundus images.[14,15]

The purpose of this study was to determine whether the photoreceptor abnormalities in eyes with OMD can be detected tangentially in the FD-OCT images and en face in the AO fundus images.

Subjects and methods

Subjects

Eight eyes of four patients, who were diagnosed with OMD in the Department of Ophthalmology, Osaka University School of Medicine, were studied. The diagnosis of OMD was made by the following findings: normal fundus, normal fluorescein angiography, decreased visual acuity, normal full-field ERGs for both rod and cone components, and reduced amplitude of mfERGs in the central 5 degrees. All of the patients were classified as having sporadic OMD because none reported other family members with similar visual problems. Some of the characteristics of these OMD patients are summarized in Table 1.

The research protocol was approved by the Institutional Review Board of the Osaka University Medical School, and the procedures used conformed to the tenets of the Declaration of Helsinki. After the nature and possible consequences of the study were explained, a written informed consent was obtained from all patients.

The mfERGs were recorded with the Veris Clinic system (Mayo Co., Aichi, Japan) under standardized conditions. The stimulus array consisted of 103 hexagons, and the luminance of each hexagon was alternated between 200 cd/m^2 and 5 cd/m^2. A cross sectional image of the retina was obtained by a FD-OCT (RTVue-100; Optovue Inc., Fremont, CA). Horizontal and vertical scans were made through the fovea with a scan length of 6 mm. To improve the signal-to-noise ratio, consecutive images were averaged with the built-in software.

AO fundus images

The AO fundus images were taken through pupils dilated with topical tropicamide (0.5%) and phenylephrine (0.5%)

Table 1 Clinical characteristics of examined patients

Age	Sex	Eye	Visual acuity	Spherical equivalent (D)	Progression	Scotoma size	Fundus	Fullfield ergs	OCT findings	
									IS/OS	OS
48	M	OD	20/100	-0.25	3 years	None	Normal	Normal	Severely disrupted	-
		OS	20/66	0		central 10deg	Normal	Normal	Severely disrupted	-
38	M	OD	20/66	-6.25	Unknown	Perifoveal 2.5deg	Normal	Normal	Severely disrupted	-
		OS	20/66	-6		Central 3deg	Normal	Normal	Severely disrupted	-
43	M	OD	20/100	-1.75	18 years	Central 2.5deg	Normal	Normal	Severely disrupted	-
		OS	20/100	-1.75		Central 2.5deg	Normal	Normal	Disrupted	-
46	F	OD	10/100	-2.5	6 months	Central 2.5deg	Normal	Normal	Disrupted in fovea	+
		OS	20/20	-1.75		None	Normal	Normal	Almost normal	+

Abbreviations: erg, electroretinogram; F, female; IS, inner segment; M, male; OCT, optical coherence tomography; OS, outer segment.

and the ciliary muscle paralyzed. A detailed description of the custom-built AO fundus camera has been published,[23,24] and the principle of our flood illumination AO fundus camera is similar to that reported by Roorda and Williams.[15] Briefly, the main components of the camera were a nematic liquid crystal phase modulator (LCPM: X8267-12; Hamamatsu Photonics, Hamamatsu, Japan), a Hartmann-Shack wavefront sensor (HSWS: 28 × 28 lenslets; specially made by Topcon, Co., Tokyo, Japan), and a scientific CCD digital camera (C9100-02; Hamamatsu Photonics, Hamamatsu, Japan). The wavefront sensor measured the ocular wavefront up to the eighth Zernike order, and the phase modulator compensated for the measured wavefront aberrations. The system is also equipped with coaxial, 8-degree-wide viewing optics to identify the location and orientation of the highly magnified retinal images.

The retina was illuminated with a 2-ms flash (635-nm wavelength) from a laser diode, and a retinal image was obtained with a 6-mm diameter exit pupil. The patient was instructed to fixate a target in the center of the field. Frame-averaging was performed using custom software (Topcon) to improve the quality of the image. Overlapping images were merged using Photoshop (Adobe Systems Inc., San Jose, CA).

Results

The age of the patients ranged from 38 to 48 years. The best-corrected visual acuity (BCVA) at examination ranged from 20/200 to 20/20. None of the patients had an episode of sudden loss of visual acuity. The duration of decrease of vision ranged from 3 months to 3 years; six eyes out of eight had a central relative scotoma by Goldmann perimetry.

Multifocal ERGs

The amplitudes of the mfERGs in the central area were reduced in all eyes. The area of the decreased amplitude varied among eyes (Figure 1).

FD-OCT

All eyes showed a disruption of the IS/OS line except the left eye of patient 3 who had a visual acuity of 20/20; meanwhile the IS/OS line and the third line are easily identifiable in normal control. Both eyes of patients 1 and 2 had a severe disruption of IS/OS line in the center of the fovea, and both had a low-intensity space between the elevated external limiting membrane (ELM) and the retinal pigment epithelium (RPE) (Figures 2B–2E). In patient 3, the IS/OS line and the RPE line were disrupted, and the retina was thinner (Figures 2F and 2G). The outer segment layer between the IS/OS line and RPE line of the FD-OCT images was visible only in the center of the fovea in the left eye of patient 4 (Figure 2I).

AO fundus images

The AO images showed patchy dark areas in all eyes, which disrupted the mosaic of bright spots in the fovea (Figures 3B–3H), compared with normal control (Figure 3A). This suggested a degeneration of some of the photoreceptors in this area. Nonuniform bright spots with irregular shapes and higher brightness appeared around the dark areas. In patient 3, the normal cone mosaic was replaced by dark areas, and nonuniform bright spots appeared to be all that remained (Figures 3F and 3G). In the left eye of patient

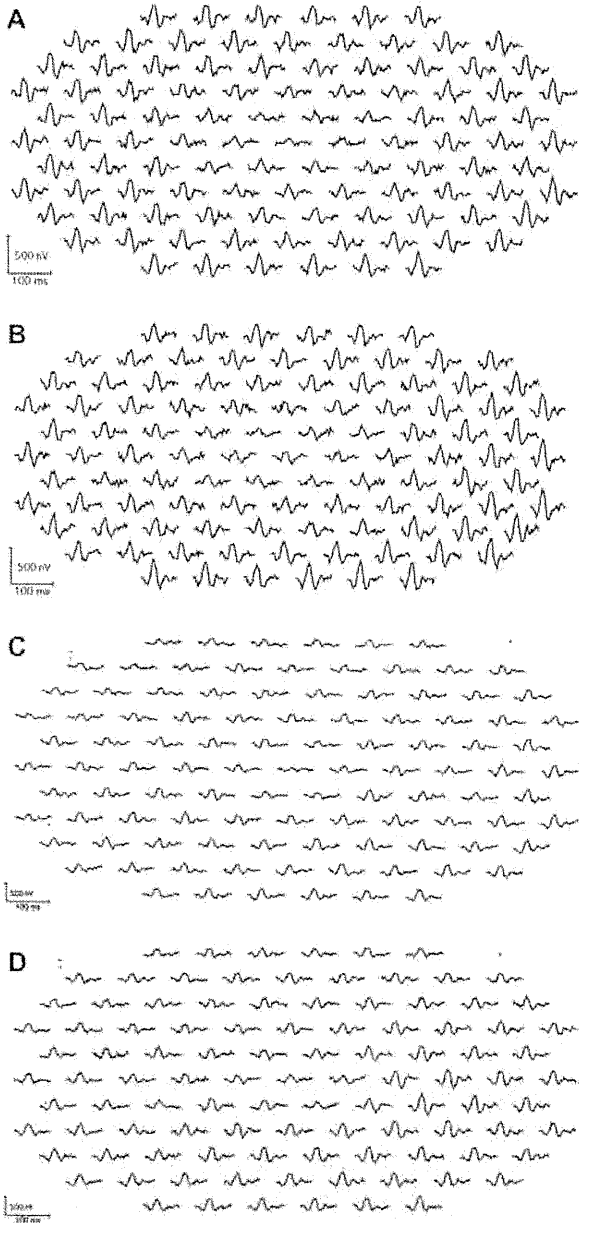

Figure 1 *(Continued)*

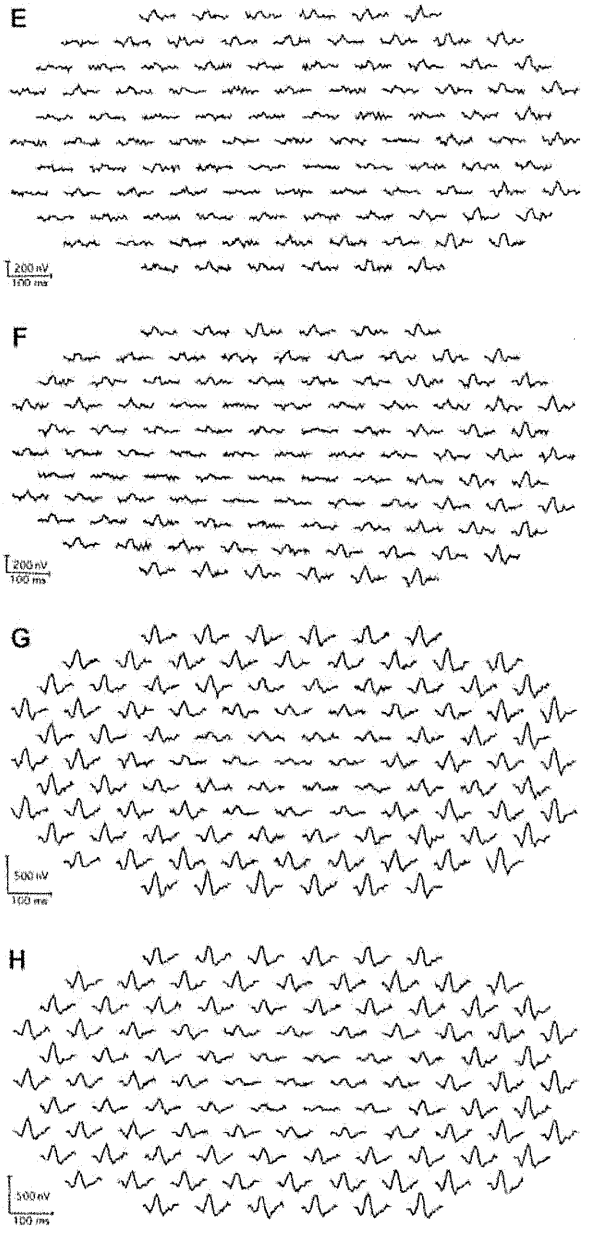

Figure 1 Multifocal electroretinogram (ERGs) of right and left eye of patient 1 (**A, B**), patient 2 (**C, D**), patient 3 (**E, F**), and patient 4 (**G, H**). Foveal amplitudes are decreased in all eyes. Especially in patient 3, amplitudes are attenuated widely including ring 5 and 6, although full-field ERG showed normal amplitude.

4, the mosaic of blight spots were in relatively good order with fewer dark areas in the center of the image (Figure 3I), although the mosaic was disrupted in the peripheral area.

Discussion

We had hypothesized that the main structures affected in eyes with OMD were the photoreceptors as in other types of retinal dystrophy, and the morphological changes of the photoreceptor could be detected by high-resolution retinal imaging techniques. This is important in eyes with OMD because histopathological sections of eyes with OMD have not

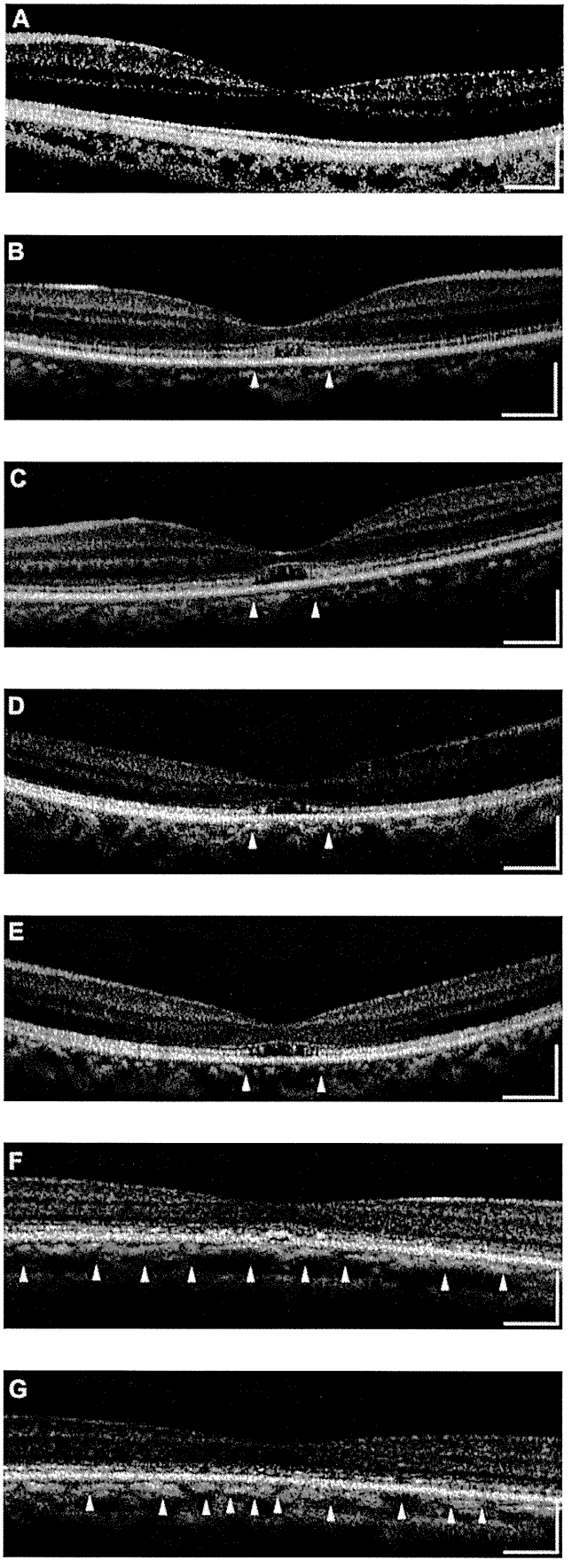

Figure 2 *(Continued)*

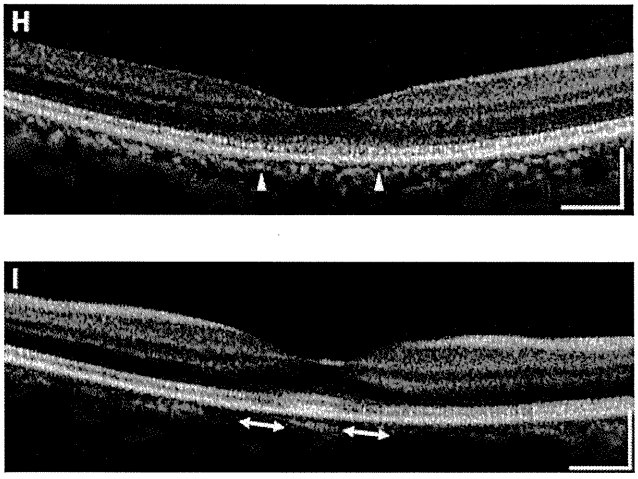

Figure 2 Fourier-domain optical coherence tomography (FD-OCT) images (horizontal scan) of normal eye (**A**), and right/left eyes of patient 1 (**B, C**), patient 2 (**D, E**), patient 3 (**F, G**), and patient 4 (**H, I**). Horizontal bars represent 500 μm, and vertical bars represent 200 μm. The eyes in patients 1–4 had a bilateral symmetric decline in visual acuity, whereas those in patient 5 had an assymmetric decline (20/200 right eye, 20/20 left eye). FD-OCT in normal eye provided clear images of the retinal layers. The external limiting membrane (ELM), photoreceptors inner and outer segment (IS/OS) junction, third line, and retinal pigment epithelium (RPE) are distinguishable. Meanwhile, the retinal photoreceptor layer is not clear in the eyes of the patients. Although ELM was visualized in all eyes, IS/OS is elevated and disrupted in fovea (**B, C, D, E, H**), widely disrupted and not clear (**F, G**), and clearly visualized in one eye (**I**). The third line was visualized only in one eye (**I**), just in the fovea.

been published. In cone-rod dystrophy, a loss of cones in the perifoveal area has been reported, and the number of cones is reduced in the extrafoveal and peripheral areas.[25,26] In addition, the length of photoreceptor outer segments has been reported to be shortened,[25,26] and an accumulation of lipofuscin granules in the RPE has also been reported in these eyes.[26]

The FD-OCT images showed a disruption of the IS/OS line and a loss of the third highly reflective line in the center of the fovea in all eyes except for the left eye of patient 4 whose BCVA was good. These findings are consistent with recent reports that there was a significant correlation between the disturbance of the IS/OS junction and the BCVA.[7,10,11]

The origin of the third bright line in the FD-OCT images has not been determined. It cannot be detected in highly myopic eyes even if the patient has good visual acuity. This suggests that the third line cannot be resolved if the length of photoreceptor outer segments is not long enough. In our patient, the third line was not detected even though they were not highly myopic. We suggest that the shortening of the photoreceptor outer segments is the reason why the third bright line cannot be seen in the FD-OCT images. However, the third line was seen in the center of the foveal area of the left eye of patient 4. In this case, we suggest that the photoreceptor outer segments were long enough in this area, and the visual acuity had not yet decreased. The AO images

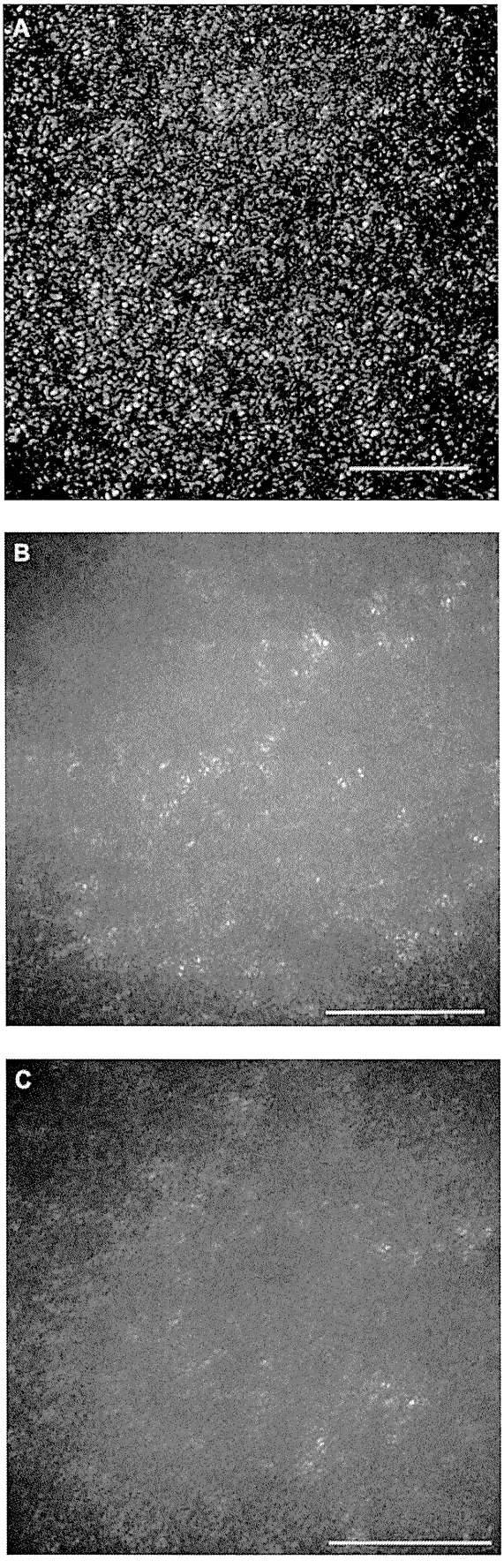

Figure 3 *(Continued)*

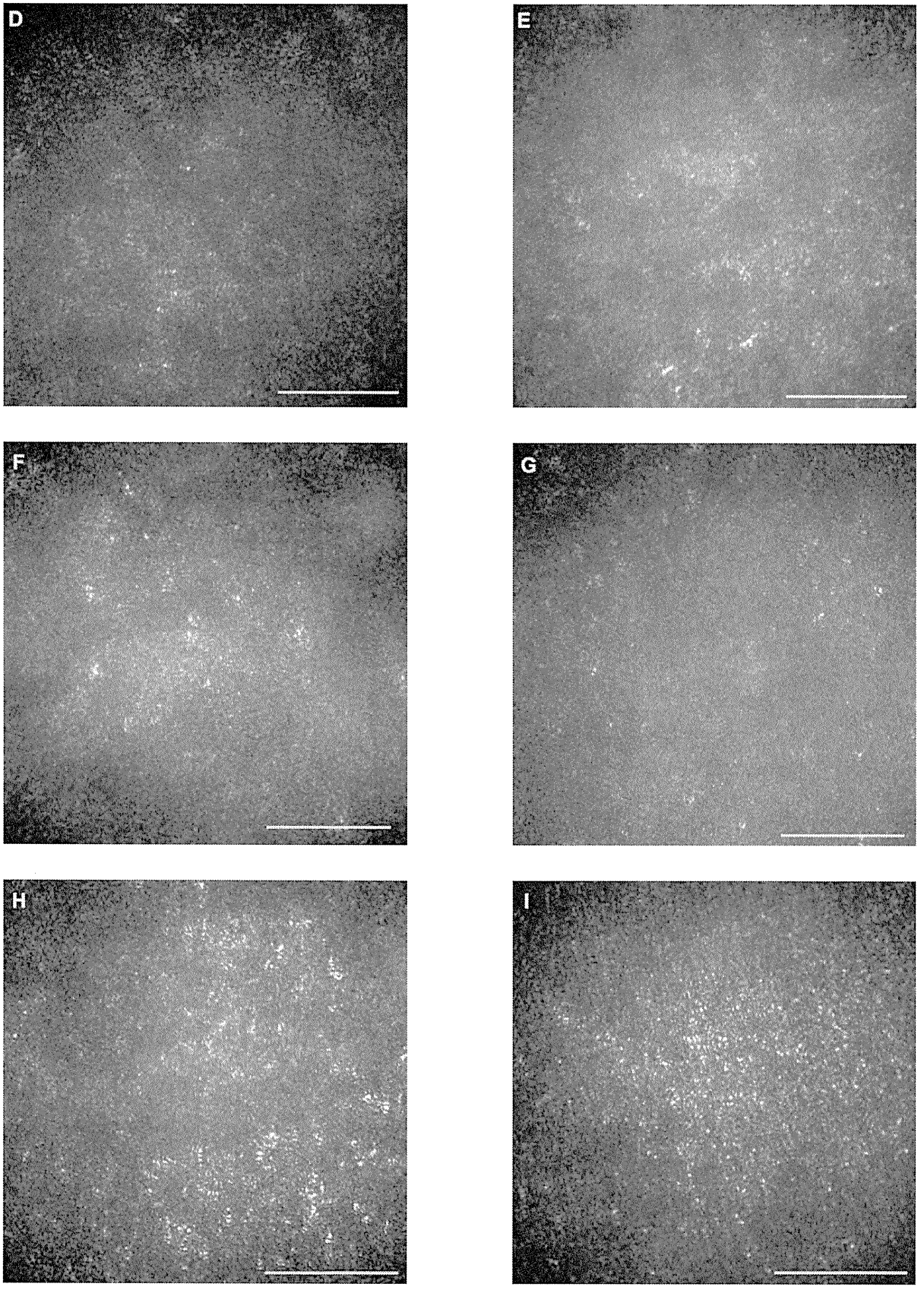

Figure 3 Adaptive optics (AO) images of the fovea of a normal eye (**A**), and right/left eyes of patient 1 (**B, C**), patient 2 (**D, E**), patient 3 (**F, G**), and patient 4 (**H, I**). Bars represent 100 μm. In the eyes of the patients, signals from the cone mosaic were attenuated, and the bright spots were distorted (**B–H**). One eye which had normal visual acuity had an almost normal appearance in the foveal center, with some dark areas around the fovea.

showed the lateral extent of the photoreceptor changes with patchy dark areas and irregular bright spots around the foveal center. There are reports of the AO findings in patients with cone-rod dystrophy (CRD) with increased cone spacing.

Until now, ophthalmologists could detect photoreceptor degeneration only by conventional ophthalmoscopy and electroretinography. In OMD patients, the photoreceptor damage is mild, and it cannot be detected by conventional ophthalmoscopy. The mfERGs are useful for detecting reduced cone function, although the result of mfERGs may be unreliable in subjects with fixation problems, such as young children and patients with eccentric fixation.[27] FD-OCT and AO are noninvasive and effective methods to observe photoreceptor damage and confirm a diagnosis.

The future applications of AO fundus examinations include monitoring disease progression and measuring the effect of treatment. Further investigations are needed to interpret and quantify the features of these images.

In conclusion, the morphological changes of OMD patients can be seen tangentially by FD-OCT and en-face by AO.

This study was supported by Health Sciences Research Grants (H19-sensory-001) from the Ministry of Health, Labor and Welfare, and by Grants (19209053) from the Ministry of Education, Culture, Sports, Science and Technology, Japan.

Disclosure

The authors report no conflicts of interest in this work.

References

1. Miyake Y, Horiguchi M, Tomita N, et al. Occult macular dystrophy. *Am J Ophthalmol*. 1996;122(5):644–653.
2. Piao CH, Kondo M, Tanikawa A, et al. Multifocal electroretinogram in occult macular dystrophy. *Invest Ophthalmol Vis Sci*. 2000;41(2): 513–517.
3. Fujii S, Escaño MF, Ishibashi K, et al. Multifocal electroretinography in patients with occult macular dystrophy. *Br J Ophthalmol*. 1999;83(7): 879–880.
4. Kondo M, Ito Y, Ueno S, Piao CH, et al. Foveal thickness in occult macular dystrophy. *Am J Ophthalmol*. 2003;135(5):725–728.
5. Brockhurst RJ, Sandberg MA. Optical coherence tomography findings in occult macular dystrophy. *Am J Ophthalmol*. 2007;143(3):516–518.
6. Drexler W, Sattmann H, Hermann B, et al. Enhanced visualization of macular pathology with the use of ultrahigh-resolution optical coherence tomography. *Arch Ophthalmol*. 2003;121(5):695–706.
7. Schocket LS, Witkin AJ, Fujimoro JG, et al. Ultrahigh-resolution optical coherence tomography in patients with decreased visual acuity after retinal detachment repair. *Ophthalmology*. 2006;113(4):666–672.
8. Alam S, Zawadzki R, Choi S, et al. Clinical application of rapid serial Fourier-domain optical coherence tomography for macular imaging. *Opthalmology*. 2006;113(8):1425–1431.
9. Ergun E, Hermann B, Wirtitsch M, et al. Assessment of central visual function in Stargardt disease/fundus flavimaculatus with ultrahigh-resolution optical coherence tomography. *Invest Ophthalmol Vis Sci*. 2005;46(1):310–316.
10. Ojima Y, Hangai M, Sasahara M, et al. Three-demensional imaging of the foveal photoreceptor layer in central serous chorioretinopathy using high-speed optical coherence tomography. *Ophthalmology*. 2007;114(12):2197–2207.
11. Piccolino FC, de la Longrais RR, Ravera G, et al. The foveal photoreceptor layer and visual acuity loss in central serous chorioretinopathy. *Am J Ophthalmol*. 2005;139(1):87–99.
12. Iida T, Hagimura N, Sato T, et al. Evaluation of central serous chorioretinopathy with optical coherence tomography. *Am J Ophthalmol*. 2000;129(1):16–20.
13. Kitaguchi Y, Fujikado T, Bessho K, et al. Adaptive optics fundus camera to examine localized changes in the photoreceptor layer of the fovea. *Ophthalmology*. 2008;115(10):1771–1777.
14. Liang J, Williams DR, Miller DT. Supernormal vision and high resolution retinal imaging through adaptive optics. *J Opt Soc Am A Opt Image Sci Vis*. 1997;14(11):2884–2892.
15. Kitaguchi Y, Fujikado T, Kusaka S, et al. Imaging of titanium:sapphire laser retinal injury by adaptive optics fundus imaging and Fourier-domain optical coherence tomography. *Am J Ophthalmol*. 2009;148(1):97–104.e2.
16. Roorda A, Williams DR. The arrangement of three cone classes in the living human eye. *Nature*. 1999;397(6719):520–522.
17. Roorda A, Williams DR. Optical fiber properties of individual human cones. *J Vis*. 2002;2(5):404–412.
18. Roorda A, Romero BF, Donnelly WJ, et al. Adaptive optics scanning laser ophthalmoscopy. *Opt Express*. 2002;10(9):405–412.
19. Pallikaris A, Williams DR, Hofer H, et al. The reflectance of single cones in the living human eye. *Invest Ophthalmol Vis Sci*. 2003;44(10): 4580–4592.
20. Wolfing JI, Chung M, Carroll J, et al. High-resolution retinal imaging of cone-rod dystrophy. *Ophthalmology*. 2006;113(6):1019.e1.
21. Duncan JL, Zhang Y, Gandhi J, et al. High-resolution imaging with adaptive optics in patients with inherited retinal degeneration. *Invest Ophthalmol Vis Sci*. 2007;48(7):3283–3291.
22. Choi SS, Double N, Hardy JL, et al. In vivo imaging of the photoreceptor mosaic in retinal dystrophies and correlations with visual function. *Invest Ophthalmol Vis Sci*. 2006;47(5):2080–2092.
23. Kitaguchi Y, Bessho K, Yamaguchi T, et al. In vivo measurements of cone photoreceptor spacing in myopic eyes from images obtained by adaptive optics fundus camera. *Jpn J Ophthalmol*. 2007;51(6):456–461.
24. Yamaguchi T, Nakazawa N, Bessho K, et al. Adaptive optics fundus camera using a liquid crystal phase modulator. *Optical Review*. 2008; 15(3):173–180.
25. Rabb MF, Tso MO, Fishman GA. Cone-rod dystrophy. A clinical and histopathologic report. *Ophthalmology*. 1986;93(11):1443–1451.
26. Demirci FY, Gupta N, Radak AL, et al. Histopathologic study of X-linked cone-rod dystrophy (CORDX1) caused by a mutation in the RPGR exon ORF15. *Am J Ophthalmol*. 2005;139(2):386–388.
27. Kondo M, Miyake Y, Horiguchi M, et al. Clinical evaluation of multifocal electroretinogram. *Invest Ophthalmol Vis Sci*. 1995;36(10):2146–2150.

Mutations in the *TSPAN12* Gene in Japanese Patients with Familial Exudative Vitreoretinopathy

HIROYUKI KONDO, SHUNJI KUSAKA, AKI YOSHINAGA, EIICHI UCHIO, AKIHIKO TAWARA, KENSHI HAYASHI, AND TOMOKO TAHIRA

• PURPOSE: To search for mutations in the *TSPAN12* gene in 90 Japanese probands with familial exudative vitreoretinopathy (FEVR) and their family members and to determine the types and frequencies of the mutations.

• DESIGN: Laboratory investigation and clinical case analyses.

• METHODS: Direct sequencing after polymerase chain reaction of the coding exons of *TSPAN12* was performed for 90 probands with FEVR and some of their family members. The clinical signs and symptoms that were characteristic of individuals with *TSPAN12* mutations were determined.

• RESULTS: Three families were found to carry 2 mutations in *TSPAN12*. One of these mutations was a new missense change, L245P, and the other was an already reported nonsense mutation, L140X, in 2 families. Mutations in *TSPAN12* accounted for 3% of Japanese FEVR patients and 8% of the FEVR families who did not have mutations in any of the known FEVR genes, *FZD4*, *LRP5*, and *NDP*. The clinical signs and symptoms varied among the patients, but the retinal findings with *TSPAN12* mutations were not different from those with mutations in the known FEVR-causing genes.

• CONCLUSIONS: Mutant *TSPAN12* is responsible for approximately 3% of FEVR patients in Japan. The results provide further evidence that mutations in *TSPAN12* are FEVR causing and that the gene products most likely play a role in the development of retinal vessels. (Am J Ophthalmol 2011;151:1095–1100. © 2011 by Elsevier Inc. All rights reserved.)

FAMILIAL EXUDATIVE VITREORETINOPATHY (FEVR) IS a hereditary disorder that is characterized by defects in the development of retinal vessels and is manifested by different retinal pathologic features, including retinal folds and retinal detachments.[1,2] The expressivity of the disease differs widely between and within families. Most individuals remain asymptomatic, and the consistent signs of FEVR are abnormal retinal vessels and avascularization of the peripheral retina.[2]

FEVR is genetically heterogeneous, and 3 genes are known to be responsible for FEVR. Mutations in the genes coding for the Wnt receptor pair, frizzled-4 (*FZD4*), and low-density lipoprotein receptor-like protein 5 (*LRP5*), are known to cause FEVR.[3,4] Mutations in genes coding for the ligand of the receptor pair, norrin (*NDP*), also cause FEVR and Norrie disease (ND).[5] The ligand–receptor complex activates canonical Wnt signaling and controls vascular development in the retina.[6] Mutations in *FZD4* cause autosomal dominant FEVR, mutations in *LRP5* cause autosomal dominant or recessive FEVR, and mutations in *NDP* cause X-linked recessive FEVR.[3–7]

Recently, a transmembrane protein, TSPAN12, was found to be expressed in the retinal vascular endothelial cells and to enhance Wnt signaling through FZD4 and LRP5.[8] This study was followed by 2 studies that demonstrated 9 mutations of this gene in autosomal dominant FEVR patients.[9,10] Because of our interest in the genetic basis of FEVR, we have examined our Japanese patients with FEVR to determine whether *TSPAN12* mutations were present in them. We show that mutations in the *TSPAN12* gene were found in only approximately 3% of the Japanese FEVR patients.

METHODS

• PARTICIPANTS AND CLINICAL EXAMINATIONS: Ninety probands, 39 familial and 51 simplex, with FEVR and 7 cases with ND were studied. All patients were Japanese and were born at term of normal weight. The diagnosis of FEVR was based on the presence of peripheral retinal avascularization with abnormal retinal vascular changes as well as the other typical clinical signs: severe retinal exudates, retinal neovascularization, peripheral fibrovascular mass, ectopic macula, retinal folds, and retinal detachment. The diagnosis of ND was made for boys who had bilateral retinal detachment or retinal folds with retrolental fibrous tissue and blindness within the first year of life. Ocular examinations included refraction, visual acuity, intraocular pressure, slit lamp, fundus, and ultrasonog-

Accepted for publication Nov 19, 2010.

From the Department of Ophthalmology, University of Occupational and Environmental Health Japan, Kitakyushu, Japan (H.K., A.T.); the Department of Ophthalmology, Fukuoka University, Fukuoka, Japan (H.K., E.U.); the Department of Ophthalmology, Sakai Hospital Kinki University Faculty of Medicine, Sakai, Japan (S.K.); the Division of Genome Analysis, Medical Institute of Bioregulation, Kyushu University, Fukuoka, Japan (A.Y., T.T.); and the Faculty of Agriculture, Kyushu University, Fukuoka, Japan (K.H.).

Inquiries to Hiroyuki Kondo, 1-1, Iseigaoka, Yahatanishiku, Kitakyushu 807-8555, Japan; e-mail: kondohi@med.uoeh-u.ac.jp

0002-9394/$36.00
doi:10.1016/j.ajo.2010.11.026

TABLE 1. Sequences of Polymerase Chain Reaction Primers Used to Amplify *TSPAN12* Coding Exons

Exon	Primer		PCR Product Size (bp)
	Forward (5′→3′)	Reverse (5′→3′)	
2	attGGTGAGATGTCCCGTGTTCT	gtTAATGCTTAGCCATGCCCTT	270
3	aTTTCAAGATGCAGCAAATGG	GTTGCTATGGGCAGGAAAAA	333
4	atTGCTATGTCTTGGGTGCATT	gttAAACGAAAGCGTCCCTTCTT	331
5	aTTTCCCCATCTGCTTCTGAG	gttAAAAGGCTGAACTGTTGTTTTAGA	267
6	attGAGCTACAGCTGTTGATATTTTGC	gttAAACATCTGGTTTGAAGGTGC	210
7	atTGATGACAGATATAGCTCTGGGT	gttGGAAAATTTCATTGGCATATTG	346
8	attGCTTTCCCTGAGAACCACTG	gtTGCTTAGGTGTTATTTTATGGCAA	574

PCR = polymerase chain reaction.

The 5′-end of each primer was designed to have an ATT or GTT for postlabeling purposes.[12] When necessary, extra nucleotides (lowercase) were attached.

raphy. Fluorescein angiography was performed on 20 probands.

• LABORATORY STUDIES: Deoxyribonucleic acid samples were extracted from peripheral blood using a deoxyribonucleic acid extraction kit (QiaAmp; Qiagen, Chatsworth, California, USA). To identify mutations in the coding exons (exons 2 to 8) of the *TSPAN12* gene, oligonucleotide primers on the flanking intron and untranslated region sequences were designed (Table 1). Polymerase chain reaction and sequencing were conducted as described.[11] The annealing temperature for polymerase chain reaction was 60 C for all exons. After sequence changes were detected in the probands, samples from other family members were analyzed by direct sequencing as well as denaturing high-performance liquid chromatography. Before this study, mutations in 3 genes, *FZD4*, *LRP5*, and *NDP*, known to cause FEVR had been analyzed in these patients.[11,12]

RESULTS

TWO NEW NONSYNONYMOUS SEQUENCE CHANGES IN THE coding sequence of the *TSPAN12* gene were found in 2 probands from Families 1 and 2 with autosomal dominant FEVR (Figure 1): c.734T→C (L245P) and c.154G→C (E52Q). L245 is located at the C-terminal cytoplasmic tail region and could provide specific functional links to cytoskeletal or signaling proteins.[13] E52 is located in the short extracellular loop. Both residues and the surrounding regions were conserved in humans and other vertebrates (Figure 1).

None of the sequence changes were found in 380 chromosomes from 190 healthy volunteers. Direct sequencing as well as denaturing high-performance liquid chromatography analysis revealed that both changes were transmitted heterozygously and were cosegregated with the disease except for a sister of the proband in Family 2 (Figure 1). This patient was diagnosed with FEVR because of abnormal retinal vessels with vitreous degeneration, but did not have the E52Q change. Therefore, we could not conclude that E52Q is responsible for FEVR.

One recurrent mutation c.419T→A (L140X) also was found in a sporadic patient (Family 3) and in a proband with autosomal dominant FEVR (Family 4). The mutation in Family 4 was reported previously.[10] Subsequent analysis of family members revealed a total of 6 mutations when the E52Q change was excluded (Figure 1). The clinical symptoms varied among the patients carrying the *TSPAN12* mutations from mild vascular changes with retinal degeneration to severe bilateral retinal folds (Table 2 and Figure 2). The clinical signs and symptoms of patients with the *TSPAN12* mutation were not different from those with mutations in known FEVR-causing genes.

Thirty-three FEVR patients who carried mutations either in *FZD4* or *LRP5* had no mutations in *TSPAN12*. Seven ND patients who had been shown to carry mutations in *NDP* had no mutations in *TSPAN12*. Thus, *TSPAN12* mutations may not be responsible for typical ND.

In addition, we found 3 known polymorphisms, 2 new nucleotide changes in introns, and 1 new synonymous nucleotide change in *TSPAN12*: IVS2-23G→A, c.91A→G, IVS6-80T→A, IVS7-81A→G (rs17142959), c.765G→T (rs41623), and c.*39C→T (rs41622). These were not considered to be responsible for FEVR.

DISCUSSION

WE EXAMINED 90 JAPANESE PATIENTS WITH FEVR FOR MUtations in the *TSPAN12* gene. Two patients with familial FEVR and 1 with sporadic FEVR were found to carry heterozygous mutations in *TSPAN12*. Our data indicated

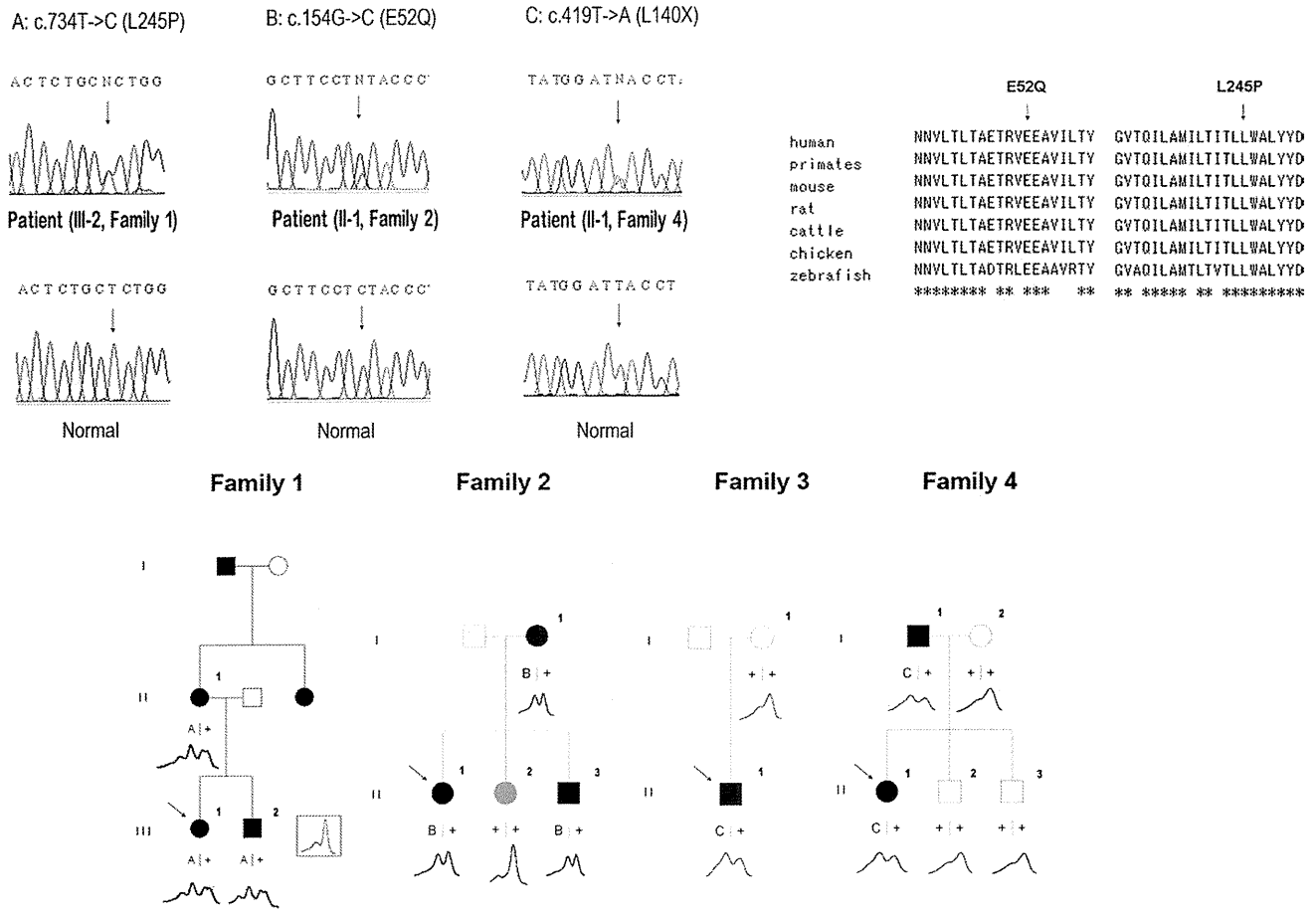

FIGURE 1. Chromatograms and pedigrees of 4 families with familial exudative vitreoretinopathy. (Top left) Mutations and nonsynonymous changes in the *TSPAN12* genes in patients with familial exudative vitreoretinopathy. Arrows indicate the positions of the altered nucleotides. E52Q is shown in the antisense direction. (Top right) Protein sequence alignment of TSPAN12 with homologues from human and other vertebrates with arrows indicating the amino acid changes. Sequence data were derived from GenBank or SwissProt based on a previous study (Poulter and associates[10]). Asterisks (*) indicate highly conserved amino acids. (Bottom) Pedigrees of 4 families illustrating the cosegregation of the *TSPAN12* mutations with familial exudative vitreoretinopathy in Families 1 through 4. Solid symbols indicate individuals with a diagnosis of familial exudative vitreoretinopathy. Arrows indicate probands. Individuals from whom sequence data were obtained are numbered. A, B, and C indicate the sequence changes L245P, E52Q, and L140X, respectively, which also are indicated above the trace data at the top. Plus (+) indicates a wild-type sequence. Results of denaturing high-performance liquid chromatography (DHPLC) are shown below each genotype. For Family 1, a wild-type pattern of DHPLC is shown in the Inset because deoxyribonucleic acid for an unaffected individual is unavailable. Note that a sister of the proband of Family 2 (filled with gray) was diagnosed with mild familial exudative vitreoretinopathy, but did not carry the mutation in *TSPAN12*. The mutation in Family 4 has been reported previously.[10]

that mutations in *TSPAN12* accounted for 3% of Japanese families with FEVR and 8% of the families in which no mutations were found in any of the genes known to be responsible for FEVR.

Our findings confirm 2 recent studies that reported that *TSPAN12* causes FEVR. Both reports showed that mutations in *TSPAN12* accounted for approximately 10% of mainly white patients in whom mutations have not been identified in the known genes.[9,10] Thus, the frequencies of mutations in this gene are similar in the 2 populations.

TSPAN12 is one of the members of tetraspanin superfamily. These proteins share 2 highly conserved features; the 4 transmembrane domains contain well-conserved residues, and the second extracellular loop has a Cys-Cys-Gly sequence and additional cysteines (Figure 3). Tetraspanins are known to participate in a spectrum of membrane-associated activities involving cell adhesion, cell proliferation, and activation of signaling pathway.[14] These proteins not only build homomultimer but also bind specifically and directly to other proteins.[15] *TSPAN12* interacts specifically with Norrin or *LRP5* and enhances the mutlimerization of the norrin/FZD4/LRP5 complex in the retina.[8] Defective *TSPAN12* possibly causes a reduction in norrin/FZD4/LRP5 signaling, which controls the angiogenic program.

TABLE 2. Mutations in *TSPAN12* Gene and the Associated Clinical Findings in Patients with Familial Exudative Vitreoretinopathy

Family	ID[a]/Age (yo)/Sex	Sequence Change	Visual Acuity (Refraction)	Peripheral Avascular Retina	Retinal Vessels Abnormality	Vitreous Degeneration	Ectopic Macula	Fibrous Tissue	Falciform Retinal Fold	Comments
1	II-1/37/F	L245P	1.2 (nc) BE	BE	BE	BE	No	No	No	
	III:1/15/F (proband)	L245P	0.06 (−2.5 D) RE; 0.6 (−6.0 D) LE	BE	BE	BE	No	RE	RE	PHC LE
	III:2/13/M	L245P	1.2 (nc) BE	BE	BE	BE	No	No	No	
3	II-1/11/M (proband)	L140X	NLP RE; 0.1 (+13.0 D) LE	LE[b]	LE[b]	NA	No	BE	BE	VxLx BE at 1 yo, phthisical RE, aphakic BE
4	I-1/42/M	L140X	1.2 (−4.0 D) BE	BE	BE	No	No	No	No	
	II-1/12/F (proband)	L140X	0.07 (+18.0 D); 0.1 (+18.0 D)	BE	BE	NA	BE	BE	No	VxLx BE at 0 yo, aphakic BE

BE = both eyes; D = diopters; Esx = esotropia operation; F = female; LE = left eye; Lx = lensectomy; M = male; NA = not analyzed; nc = not correctable; PHC = photocoagulation; RE = right eye; Vx = vitrectomy; yo = year(s) old.

[a]Identifications are referable to Figure 1, Bottom.

[b]Findings on the right eye were not available because of phthisis.

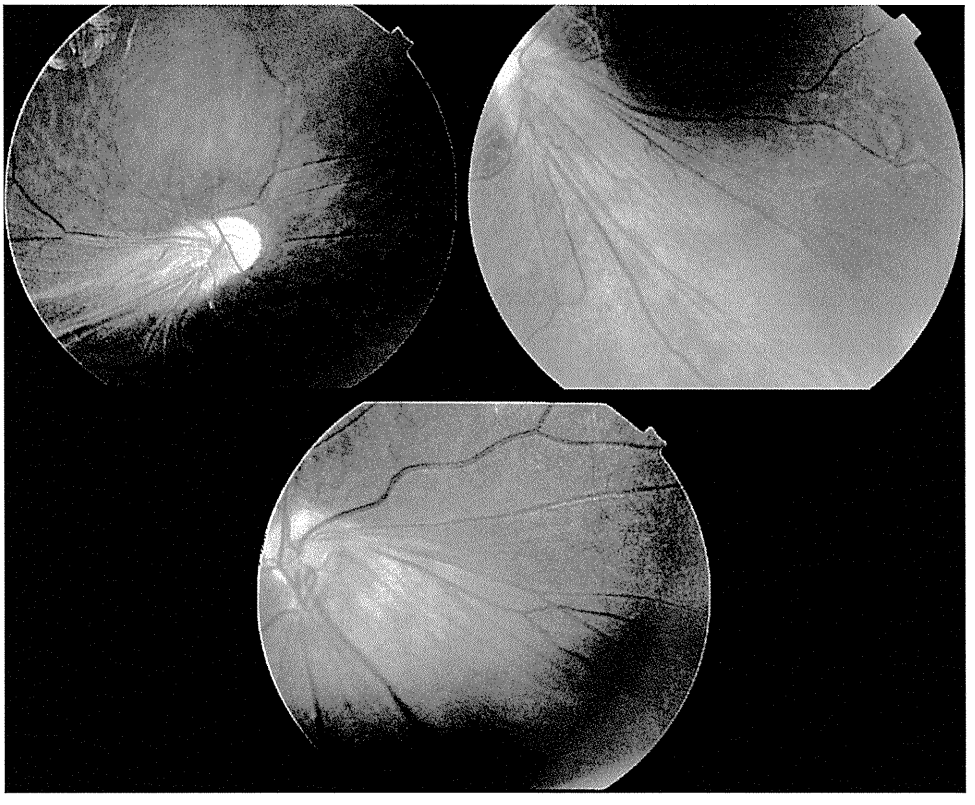

FIGURE 2. Fundus photographs of patients with familial exudative vitreoretinopathy carrying mutations in *TSPAN12*. (Top left) Fundus photograph of the right eye of the proband of Family 1 showing a retinal fold resulting from retrolental fibrous tissues. (Top right and Bottom) Fundus photographs of the left eyes of the probands of Families 3 and 4 showing a dragged macula.

So far, 9 mutations in *TSPAN12* have been identified (Figure 3). Of these mutations, at least 5 (insertion, deletion, nonsense, and splicing) are predicted to result in truncated proteins that may not be synthesized because of nonsense-mediated decay of the messenger ribonucleic acid.[10] One missense mutation, A237P, was suggested to be subjected to proteolytic degradation.[9] Based on these data, haploinsufficiency of *TSPAN12* was proposed as the cause of FEVR.

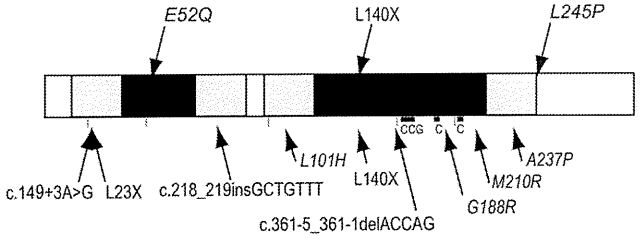

FIGURE 3. Schematic diagram of the structure of TSPAN12 and locations of mutations and nonsynonymous change identified in the *TSPAN12* gene in familial exudative vitreoretinopathy patients. TSPAN12 contains 4 transmembrane domain (shaded boxes), and the first and second extracellular loop domains (filled boxes) are highly conserved. White boxes indicate intracellular regions. Vertical bars indicate exon–intron boundaries. Horizontal bars indicate a conserved Cys-Cys-Gly sequence (CCG) and the partner cysteins (C) that form disulfide bridges. One nonsense mutation and 2 nonsynonymous sequence changes identified in this study are at the top. Note that E52Q did not cosegregate with disease and may not be responsible for familial exudative vitreoretinopathy (asterisk). Mutations previously reported by Nikopoulos and associates and Poulter and associates are at the bottom.[9,10] Missense mutations are shown in italics.

The expression of the clinical features of the patients with *TSPAN12* mutations differed widely, as shown in Table 2 and Figure 2. The probands showed relatively severe retinopathy, for example, retinal folds, whereas the other family members often were asymptomatic, as has been reported in individuals who carry mutations in other FEVR-causing genes. The retinal findings in patients with *TSPAN12* mutations were not different from those with mutations in *FDZ4* and *LRP5*,[10] although retinal exudates were not found in our patients. Mutations in *LRP5* are known to cause reduced bone density,[11] but we did not examine the systemic changes in the patients with *TSPAN12* mutations in detail.

For Family 2, a change in E52Q was found in 3 individuals with FEVR, whereas the same change was not found in a sister of the proband who also had mild FEVR. The lack of cosegregation suggests that E52Q is a nonpathogenic polymorphism. However, the genetic background of FEVR is likely to be more complex than that of Mendelian pedigree patterns.[11,16] A possibility remains that this family has an unknown genetic background that may make them susceptible to the disease depending on the E52Q change. Functional analysis is required to assess the effect of this change.

In conclusion, we examined 90 patients with FEVR for mutations in the *TSPAN12* gene, and 3 families were found to carry heterozygous mutations in *TSPAN12*. These findings indicate that mutant *TSPAN12* is responsible for approximately 3% of FEVR in Japan. The results provide additional evidence that mutations in *TSPAN12* are FEVR causing that and *TSPAN12* is crucial for the development of the retinal vessels.

PUBLICATION OF THIS ARTICLE WAS SUPPORTED BY THE JAPAN SOCIETY FOR THE PROMOTION OF SCIENCE, TOKYO, JAPAN (Grants-in-Aid for Scientific Research 22591956), and the Ministry of Health, Labour and Welfare of Japan (Grants for Research on Intractable Diseases 22141101). The authors indicate no financial conflict of interest. Involved in Design of study (H.K., T.T.); Conduct of study (H.K., S.K., K.H.); Data collection (H.K., A.Y.); Analysis and interpretation of data (H.K., T.T., K.H.); Writing and preparation of the manuscript (H.K.); Review and approval of the manuscript (E.U., A.T.). The procedures used conformed to the tenets of the Declaration of Helsinki. Informed consent was obtained from all patients, and the experimental protocol was approved by the Ethics Review Board of Fukuoka University. The authors thank the patients and their families and Duco Hamasaki, Professor Emeritus, Bascom Palmer Eye Institute, University of Miami, Miami, Florida, for his critical comments and valuable assistance.

REFERENCES

1. Criswick VG, Schepens CL. Familial exudative vitreoretinopathy. Am J Ophthalmol 1969;68(4):578–594.
2. Warden SM, Andreoli CM, Mukai S. The Wnt signaling pathway in familial exudative vitreoretinopathy and Norrie disease. Semin Ophthalmol 2007;22(4):211–217.
3. Robitaille J, MacDonald ML, Kaykas A, et al. Mutant frizzled-4 disrupts retinal angiogenesis in familial exudative vitreoretinopathy. Nat Genet 2002;32(2):326–330.
4. Toomes C, Bottomley HM, Jackson RM, et al. Mutations in LRP5 or FZD4 underlie the common familial exudative vitreoretinopathy locus on chromosome 11q. Am J Hum Genet 2004;74(4):721–730.
5. Chen ZY, Battinelli EM, Fielder A, et al. A mutation in the Norrie disease gene (NDP) associated with X-linked familial exudative vitreoretinopathy. Nat Genet 1993;5(2):180–183.
6. Xu Q, Wang Y, Dabdoub A, et al. Vascular development in the retina and inner ear: control by Norrin and Frizzled-4, a high-affinity ligand-receptor pair. Cell 2004;116(6):883–895.
7. Jiao X, Ventruto V, Trese MT, Shastry BS, Hejtmancik JF. Autosomal recessive familial exudative vitreoretinopathy is associated with mutations in LRP5. Am J Hum Genet 2004;75(5):878–884.
8. Junge HJ, Yang S, Burton JB, et al. TSPAN12 regulates retinal vascular development by promoting Norrin- but not Wnt-induced FZD4/beta-catenin signaling. Cell 2009;139(2):299–311.
9. Nikopoulos K, Gilissen C, Hoischen A, et al. Next-generation sequencing of a 40 Mb linkage interval reveals TSPAN12 mutations in patients with familial exudative vitreoretinopathy. Am J Hum Genet 2010;86(2):240–247.
10. Poulter JA, Ali M, Gilmour DF, et al. Mutations in TSPAN12 cause autosomal-dominant familial exudative vitreoretinopathy. Am J Hum Genet 2010;86(2):248–253.
11. Qin M, Hayashi H, Oshima K, Tahira T, Hayashi K, Kondo H. Complexity of the genotype-phenotype correlation in familial exudative vitreoretinopathy with mutations in the LRP5 and/or FZD4 genes. Hum Mutat 2005;26(2):104–112.

12. Kondo H, Qin M, Kusaka S, et al. Novel mutations in Norrie disease gene in Japanese patients with Norrie disease and familial exudative vitreoretinopathy. Invest Ophthalmol Vis Sci 2007;48(3):1276–1282.
13. Stipp CS, Kolesnikova TV, Hemler ME. Functional domains in tetraspanin proteins. Trends Biochem Sci 2003;28(2): 106–112.
14. Garcia-Espana A, Chung PJ, Sarkar IN, Stiner E, Sun TT, Desalle R. Appearance of new tetraspanin genes during vertebrate evolution. Genomics 2008;91(4):326–334.
15. Hemler ME. Tetraspanin functions and associated microdomains. Nat Rev Mol Cell Biol 2005;6(6):801–811.
16. Kondo H, Qin M, Tahira T, et al. Severe form of familial exudative vitreoretinopathy caused by homozygous R417Q mutation in frizzled-4 gene. Ophthalmic Genet 2007;28(4): 220–223.

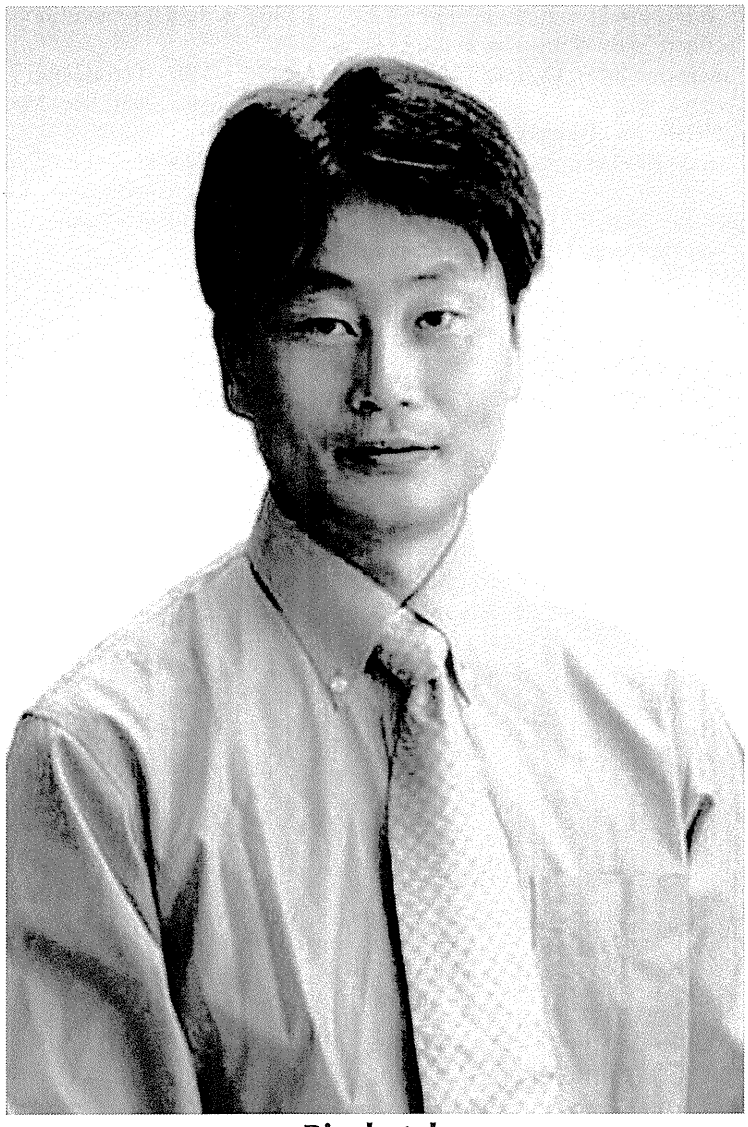

Biosketch

Hiroyuki Kondo, is an Associate Professor at the Department Ophthalmology, University of Occupational and Environmental Health, Japan. His interests include ophthalmic genetics and vitreoretinal surgery, with specialization in pediatric vitreous surgery.